https://doi.org/10.46813/2026-161-081

DISTURBANCES IN THE SURFACE STRUCTURE OF TUNGSTEN SAMPLES 99.5 AND 99.7% PURITY IRRADIATED BY 0.12 OR 4 MeV HELIUM IONS

E.M. Prokhorenko[1], O.V. Manuilenko[2], I.N. Onishchenko[2], V.V. Lytvynenko[1], B.V. Zajtsev[2], K.V. Pavlii[2], V.A. Soshenko[2], V.I. Butenko[2], T.G. Prokhorenko[3]

[1]Institute of Electrophysics and Radiation Technologies NAS of Ukraine, Kharkiv, Ukraine;
[2]NSC "Kharkiv Institute of Physics and Technology", Kharkiv, Ukraine;
[3]Kharkiv National Automobile and Highway University, Kharkiv, Ukraine
E-mail: e.m.prokhorenko@gmail.com

High-purity tungsten (99.7% (W-n) and 99.5% (W-1)), was considered as a material for creating the first wall of a thermonuclear reactor. The choice of tungsten as a promising material for the first wall was determined by its high heat-resistant characteristics, low corrosion, and high radiation resistance. To understand the effect of irradiation on the properties and characteristics of high-purity tungsten, in comparison with ceramic materials and materials from special grades of steel, of samples of tungsten were irradiated with the ions of helium with energies of E_{He}^{+} = 0.12 MeV or E_{He}^{+} = 4 MeV. The change in the structure of surface defects was investigated. It was found that the flecking processes proceed five times more efficiently than the blistering processes. It was also found that during the formation of tungsten "fluff", the thickness of separate filaments is three times less than the height. The coefficients of ionization, phonon production and vacancy appearance were calculated using mathematical modeling methods. The coefficients were found on the penetration depth of ions of helium. The total coefficients of displacements were found depending on energy of irradiation.

PACS: 52.40.HF, 29.27Ac, 621.715:539.376, 87.55N

INTRODUCTION

The use of high-purity materials allows us to solve many problems in modern energy. One of the important problems of using pure materials is their use in installations where there are various ionizing radiations. Such installations include reactors based on nuclear fusion reactions (thermonuclear reactors) [1, 2].

When creating thermonuclear reactors, it is necessary to decide on the choice of material for the first wall [3]. The materials of the first wall must have high resistance to a number of factors. The most critical of these are: a) thermal effects (>1200 K) [4], b) plasma effects [5], c) radiation effects of nuclear fusion products [6].

Thermal action results in the appearance of microscopic points of molten metal on the surface of the first wall material and the appearance of bubble boiling areas. At the same time, the material evaporates from the surface of the material and is Sputtering (sprayed) into the working volume. This leads to plasma contamination. Craters and bulges are formed on the surface of the material. The material is tempered and becomes embrittlement (embrittled).

When a fusion reactor operates, the first wall is exposed to plasma and fusion products [1–6]. Fast neutrons (14.2 MeV, ~ 2 dpa). may be present. Also, a yield of ~ 10^{24} $H^{+}m^{-2}\cdot s^{-1}$ (1…10 eV) protons and ~ $10^{22}…10^{24}$ $He^{2+}m^{-2}\cdot s^{-1}$ (<500 eV) helium ions is possible in a MFE fusion reactor. For laser-pumped IFE reactors (HAPL), deuterium fluxes with energies from 1 keV to 10 MeV may be present. Helium ion fluxes of ~ 10^{15} m^{-2} (in the range of 200 keV…10 MeV) may also appear [2–7].

The impact of the thermonuclear reaction products on the first wall enhances and accelerates the effects that arise as a result of thermal exposure.

All these changes and surface disturbances lead to changes and destruction of material of the first wall. Simultaneously with the change in macroscopic properties, the microscopic characteristics of the first wall materials also change. Thermal and radiation effects lead to the appearance, growth and migration of various defects.

In this case, the orientation of the crystal grates structure of the first wall changes. These effects (macro and micro) significantly change both thermal and mechanical properties (hardness, plasticity, etc.). Therefore, it is necessary to study how these effects affect the durability of the materials of the first wall.

Perspective materials for the first wall of a thermonuclear reactor are ceramics, steel, and tungsten [7–9]. The use of composites based on these materials is also being considered.

We focused on tungsten. He has a high melting point and high strength at these temperatures. Tungsten has significant residual strength after cooling. Tungsten has a high thermal conductivity coefficient. The coefficient of erosive spraying of tungsten is low. Also, tungsten poorly retains tritium.

Thus, tungsten has several specific properties that allow it to be used as a first wall material. Changes in the structure of tungsten under the influence of thermal and radiation factors may depend on impurities of other materials in tungsten. In the experiment, samples of tungsten (99.5% and 99.7%) were studied. They differed in individual impurities. Beams of helium with energies of 0.12 or 4 MeV were used for the studies.

PURPOSE OF WORK

The main tasks that need to be solved:

a) Perform irradiation of high-purity of samples of tungsten of 99.7% (W-n) and 99.5% (W-1).

b) Conduct simulation modeling of radiation processes using ionizing radiation (of ions of helium beams with energies of 0.12 or 4 MeV).

c) Calculate the coefficients of ionization, coefficients of photon yield, and coefficients of appearance of vacancies.

d) Conduct a comparative analysis of surface damage to samples of varying purity and at different of ions of helium energies.

THE MAIN PART

CONDUCTING EXPERIMENTS AND DISCUSSION OF RESULTS

When studying changes in the structure of tungsten, simulation modeling was performed. Accelerated charged particles were used for this purpose. The use of heavy charged particles makes it possible to model some of the processes that occur in the active zones of nuclear and thermonuclear reactors, under steady-state and transient operating conditions. Since heavy ions have a scattering cross-section five orders of magnitude greater than neutrons, it is possible to create radiation damage 10^6 greater than with neutron irradiation (Fig. 1).

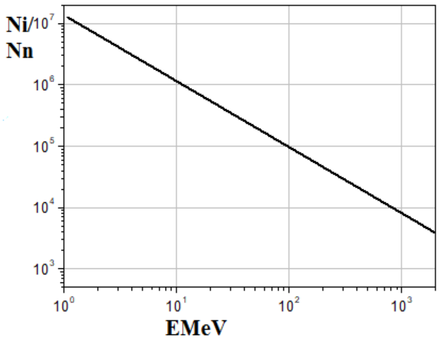

Fig. 1. Graph of changes in damage values from energies

That is, by irradiating samples for several hours with beams of heavy ions with an intensity of several microamperes, we can reproduce the radiation effect that is achieved in real nuclear installations over several years.

It should be noted that the use of beams of heavy ion allows one to avoid working with radioactive substances. It also becomes possible to conduct research in both “cold” and “hot” modes.

All experimental work was carried out using of accelerating of beams of ions of helium [10–13]. This accelerator complex allows obtaining beams of ions of helium with the following characteristics: pulse current 700 μA, pulse length 500 μs, average current 0.7 μA, repetition frequency 2…5 imp./s, current density $(0.15…0.44)\cdot10^{13}$ part./cm^2. The studies were carried out using the beams of ions of helium with energies of 4 MeV (acceleration mode) and 1.2 MeV (injection mode).

The control of thermal characteristics and vacuum condition of the equipment was carried out using IR-radiometric methods [14]. The experiments were carried out in the “cold” mode, at a temperature of 380 K. In this case, there are no defects in the samples that are caused by thermal exposure. Defects that appeared as a result of radiation exposure are studied.

Conducting research on tungsten is important because it has a wide range of applications. Tungsten is used in the manufacture of containers for storing and transporting RAW, in the construction of storage RAW [15], in the creation of radiation- shielding materials [16–20], in the manufacture of balls for drum mills, which are used in uranium mining [21–23].

For experiments [24–27] the samples of tungsten were made in the form of disks, 2 mm thick and 10 mm in diameter. Irradiation was performed perpendicular to the end. The ends of the disks were polished. This form of disks and method of irradiation allows to detect and examine structural defects, both on the side of irradiation and on the opposite side.

During the irradiation of tungsten with the beams of ions of helium, ions are implanted into the material, and the structure of the samples changes. Defects of grates appear, accumulate, and diffuse. All these disturbances lead to changes in the characteristics of the surface of tungsten.

In the experiments, samples of tungsten with a purity of 99.7% (W-n) and 99.5% (W-1) were studied [24–27].

Using X-ray fluorescence analysis techniques, the composition of samples of tungsten was determined. The numerical values of impurities are given in the works [24–27]. The samples W-1 (99.5%) have more impurities than the samples W-n (99.7%). The impurities were the following metals: Fe, Al, Cr, Ni, Co, Mo. The difference in total is 0.15%.

After irradiation, the samples were kept in stabilization conservation for three months. This is due to radiation safety requirements.

During the studies of structure of tungsten, diffractometric studies were performed. Applied the diffractometer of DRON-4-07. A photograph of the diffractogram of an unirradiated sample is shown in Fig. 2.

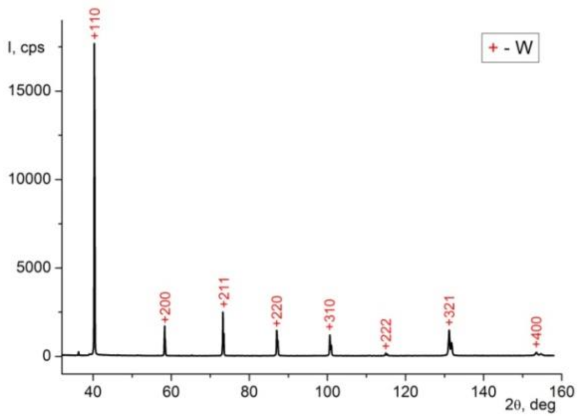

Fig. 2. Photograph of the diffractogram of the unirradiated sample of tungsten of W-n (99.7%)

Fig. 2 shows how the intensity of the reflected signal changes in the unirradiated sample of tungsten of W –n (99.7%). Phase of tungsten with the grate parameter to: a = (3.1658±3·10^{-4}) Å. There are no other phases. For tungsten of W-1 (99.5%) the grate parameter has the value: a = (3.1672±3·10^{-4}) Å.

It should be noted that the parameter of grate is affected by impurities. Impurities increase the parameter of grate. This is confirmed by the fact that for tungsten with a purity of 99.9%, the parameter of grate has a value of a = 3.1652 Å. This is less than that of samples of tungsten W-n (99.7%) and W-1 (99.5%).

In studying violations, methods of mathematical modeling are widely used. In the review [28] and the bibliography to it, it is shown that there is a high correspondence between the calculated results and experimental measurements. The importance of performing numerical modeling of the processes that occur during irradiation is noted.

In our studies, we used the SRIM code [29]. The attenuation of the ionizing radiation dose was calculated using the Geant4 v 4.9.6p02 software package [30].

Using the SRIM code, we can calculate: lengths of free run of ions in material of target, the distribution of vacancies, and the distribution of recoil atoms. Based on these values, we find the following characteristics: the amount of damage of target; the coefficient of sputtering of atoms from the surface of target; the coefficient of ionization of the material in the volume of target; the number of phonons that arose in the volume of target.

The structure changes of tungsten along the trajectory of ions of helium. The number of dislocations and loops changes. The material is ionized, phonons are formed. The results of the numerical calculation for ions with energies of 0.12 MeV are presented in Table 1 [24, 25, 27].

The characteristics of ionization and phonon appearance were obtained for samples of tungsten irradiated with ions of helium with energies E_{He} = 4 MeV. The results of the numerical calculation are presented in Table 2 [24, 26, 27].

Table 1

The values (%) of energy loss and damage of samples of tungsten W-1 (99.5%) and W-n (99.7%), when irradiated with ions of helium with energies of 0.12 MeV

Material purity	W-1 (99.5%) Energy loss, E_{He} = 0.12 MeV. Formation of vacancies = 148 vac./ion Damageability = 168 displacements/ion free run (max) = 0.5 μm			W-n (99.7%) Energy loss, E_{He} = 0.12 MeV. Formation of vacancies = 146 vac./ion Damageability = 166 displacements/ion free run (max) = 0.48 μm		
Parameters	Ionization, %	Displacements, %	Phonons, %	Ionization, %	Displacements, %	Phonons, %
Ions He+	93.99	0.08	0.58	93.98	0.08	0.74
Cascade of Displacement	1.35	0.21	3.29	1.35	0.28	3.57

Table 2

The values (%) of energy loss and damage of samples of tungsten W-1 (99.5%) and W-n (99.7%)), when irradiated with ions of helium with energies of 4 MeV

Material purity	W-1 (99.5%) Energy loss, E_{He} = 4 MeV. Formation of vacancies = 340 vac./ion Damageability = 338 displacements/ion free run (max) = 7.05 μm			W-n (99.7%) Energy loss, E_{He} = 4 MeV. Formation of vacancies = 339 vac./ion Damageability = 336 displacements/ion free run (max) = 7.00 μm		
Parameters	Ionization, %	Displacements, %	Phonons, %	Ionization, %	Displacements, %	Phonons, %
Ions He^+	99.69	0.00	0.04	99.59	0.00	0.04
Cascade of Displacement	0.10	0.02	0.24	0.10	0.02	0.24

As follows from the tables, the characteristics of the samples differ little. However, they exist. The main losses of the helium ion beam are spent on the ionization of tungsten. The radiation characteristics changes of tungsten little when exposed to displacement cascades. And a very small part of the beam of ions energy is spent on the formation of phonons.

When irradiated with ions of helium with energy of 0.12 MeV, 95% of the energy of beam is spent on ionization (see Table 1). When irradiated with ions of helium with energy of 4 MeV, 99.6% of the energy of beam is spent on ionization (see Table 2). All processes occur due to the effect of ions of helium.

The values of the changes in the following characteristics were obtained: the coefficient of ionization of the material of target, the coefficient of formation of phonon, and the coefficient of segregation (redistribution) of atoms. The changes in these values for ions with energies of 0.12 MeV were presented in the form of graphs in Fig. 3 [24, 25, 27].

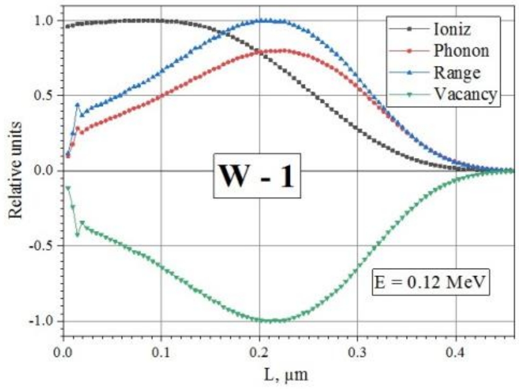

a

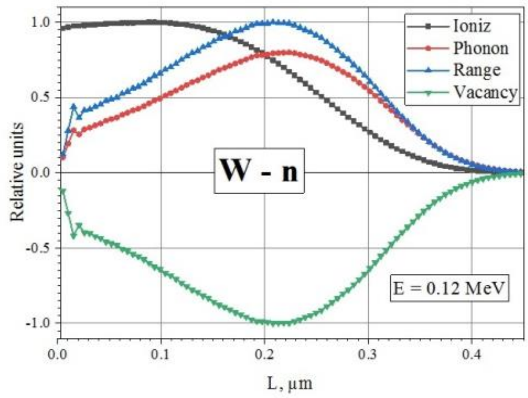

b

Fig. 3. Curves which show of changes in the number of vacancies, photons, ionization in the sample of tungsten: W-1 (99.5%) (a), W-n (99.7%) (b). Irradiation with ions of helium with energy 0.12 MeV

These samples of tungsten were irradiated with ions of helium with energies of 0.12 MeV. All processes in the samples occur to depths of 0.45 μm. For these samples, which are close in purity, the processes of ionization, segregation and formation of phonon in the same way (see graphs Fig. 3 differ insignificantly).

The maximum values of the peaks are 0.01 μm larger for the tungsten of type of W-1 (99.5%), than for the tungsten of type of W-n (99.7%). The mean free run is 0.48 μm for tungsten of W-1 (99.5%). For tungsten of W-n (99.7%), the mean free path is 0.5 μm. The half-width of peak of the production of phonon is 0.23 μm and is in the range from 0.09 to 0.32 μm.

The values of these quantities were obtained for the samples of tungsten irradiated with ions of helium with energies of 4 MeV. The results are shown in Fig. 4 [24, 26, 27].

All processes are the same for both samples. The mean of free run is 7.05 μm for the W-1 sample of tungsten of type of (99.5%). The mean free path is 7.0 μm for the W-n sample of tungsten of type of (99.7%).

Ionization processes occur along the entire of free run and end at a depth of 6.4 μm. For different types of tungsten, the difference in coefficients is equal to 0.1 μm (4 MeV). These differences arose due to the higher content of tungsten in the sample of W-n (99.7%).

The half-width of the peak of the coefficient of production of phonon is in the range of 5.8…6.3 μm (4 MeV) and is 1.5 μm. All these values are larger for the case of irradiation with ions of helium with energies of 4 MeV than for the case of irradiation with ions of helium with energies of 0.12 MeV.

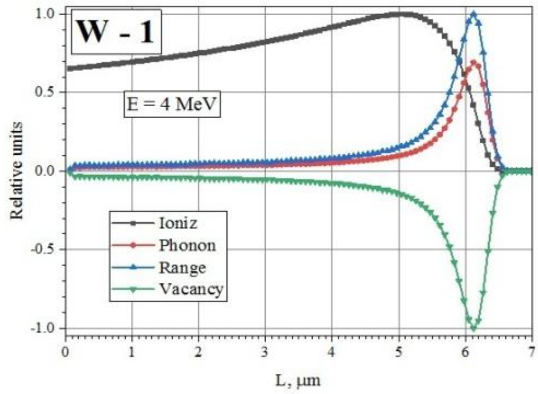

a

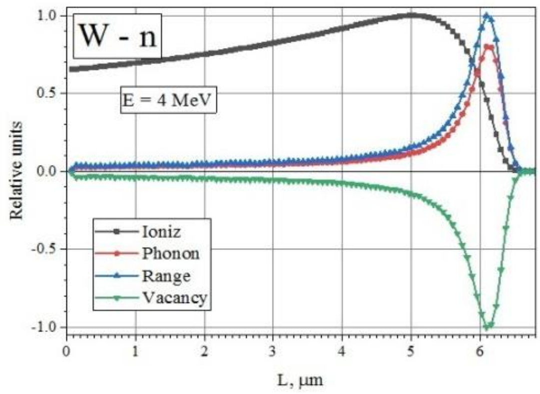

b

Fig. 4. Curves which show of changes in the number of vacancies, photons, ionization in the samples of tungsten: W-1 (99.5%) (a); W-n (99.7%)(b). Irradiation with ions of helium with energies of 4 MeV

The numerical values of the ionization coefficient, coefficient of formation of phonon, and coefficient of segregation are used to find the coefficient of displacement (dpa – the number of displacements per atom). The coefficient of displacement (dpa) was calculated using expression [25, 26, 27]:

$$dpa = \frac{D_{ion} \cdot dpi}{N_A \cdot \rho_0 \cdot SL} \cdot \frac{1}{100} \sum_i \mu_i n_i ,$$

where D_{ion} – is the radiation dose, ion/cm^2. The D_{ion} parameter is found from the experimental conditions. The *dpi* parameter is the number of displacements per ion. The *dpi* parameter is found from the total number of displacements per ion. N_A – is Avogadro's number. In this equation: ρ_0 – is the density of the sample; $S = 1$ cm^2 – is the unit area of the sample; L – is the maximal run of ions in a sample. The value $M = 1/100 \times \sum \mu_i n_i$ – is the molar mass of the sample. The value of μ_i – is the molecular weight of the *i*-th element of the sample; n_i – is the percentage of the *i*-th element of the sample.

Using calculations, graphs were obtained that display the displacement coefficients Fig. 5 [24, 25, 27].

The results are given for irradiation of samples of tungsten with ions of helium with energies E_{He+} = 0.12 MeV. The maximum of the peak of displacement is in the depth range of 0.22…0.23 μm, for the samples W-1 (99.5%) (see Fig. 5,a) The maximum of the peak of displacement is in the range of 0.21…0.22 μm, for the samples W-n (99.7%) (see Fig. 5,b).

The half-width of the displacement profile peak is in the range of 0.09…0.31 μm W-1 (99.5%) (see Fig. 5,a) and 0.08…0.31 μm W-n (99.7%) (see Fig. 5,b). At such a depth, individual ions can lead to displacements of up to 200 dpa. At depths of 0.00…0.08 μm and 0.32…0.6 μm, the maximum displacement per ion is no more than 130 dpa.

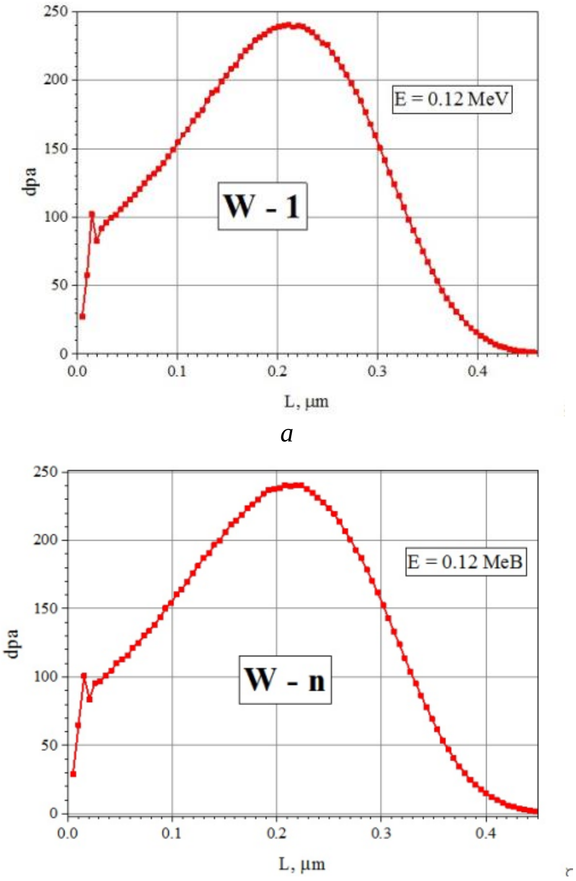

b

Fig. 5. Displacement formation profile in a samples of tungsten: W-1 (99.5%) (a), W-n (99.7%) (b). Irradiation with ions of helium with energy: E_{He^+} = 0.12 MeV

At the irradiation dose of $1 \cdot 10^{18}$ ion/cm^2, the total coefficient of displacement had the following values: dpa ≈ 60 for W-1 (99.5%), and dpa ≈ 59 for W-n (99.7%).

Graphs of the coefficient of displacement change for the samples of tungsten (W-1 (99.5%), W-n (99.7%)) were obtained [24, 26, 27] when the energy of ion was 4 MeV (see Fig. 6,a,b).

The results were obtained by irradiation with ions of helium with energies E_{He^+} = 4 MeV. For tungsten of type the W-1 (99.5%), it was found that the maximum value of the coefficient of displacement (dpa) is 9. The peak of the coefficient of displacement is at 6.2 μm (see Fig. 6,a). For tungsten of type the W -n (99.7%), it was found that the maximum value of the coefficient of displacement (dpa) is 10. The peak of the coefficient of displacement is at 6.1 μm (see Fig. 7,b).

The half-width of the displacement profile peak is in the range of 5.7…6.4 μm W-1 (99.5%) (see Fig. 7,a) and 5.8…6.3 μm W-n (99.7%) (see Fig. 6,b). At such depths, individual ions can lead to displacements of up to 10 dpa. At depths of 0.00…5.8 μm and 6.3…7.0 μm, the maximum displacement per ion is no more than 2 dpa.

At a irradiation dose of $1 \cdot 10^{18}$ ion/cm^2, the total coefficient of displacement had the following values: dpa ≈ 8.75 for W-1 (99.5%), and dpa ≈ 8.7 for W-n (99.7%).

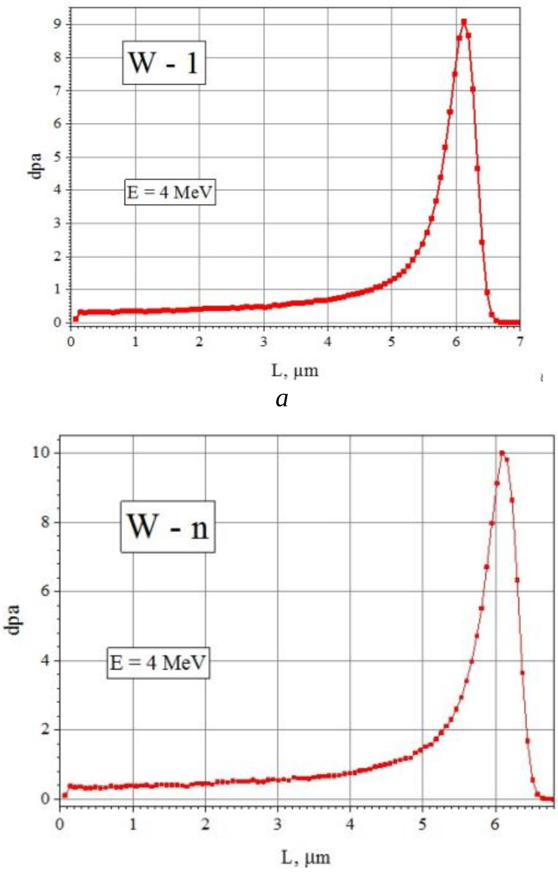

b

Fig. 6. Displacement formation profile in a samples of tungsten: W -1 (99.5%) (a), (W -n (99.7%) (b). Irradiation with ions of helium with energy: E_{He^+} = 4 MeV

The irradiation of samples was accompanied by the origin of radiation defects and appearance of radiation damages. In the case of irradiation with ions of helium with energy of 4 MeV, the radiation dose was $1.62 \cdot 10^{18}$ ion/cm^2. In this case, the dose of radiation damage was 8.1 dpa [25–27]. This dose of radiation damage in real conditions will be accumulated in a long time. When irradiated with helium ions with energies of 0.12 MeV, the radiation dose was $1.7 \cdot 10^{18}$ ions/cm^2, and the radiation damage dose was 93.78 dpa [24–27].

All differences are caused by the higher purity of the sample of W-n (99.7%) and, accordingly, a larger amount of tungsten, as compared to the sample of W-1 (99.5%).

When ions of helium the material of target, three main processes occur. One of them is implantation (insertion of ions into the crystal grate of the target).

This hardens the surface of the sample [31]. Bubbles are formed and come to the surface (flaking).

The effects of flecking and blistering are manifested [32, 33]. Diffusion of ions to the surface also occurs. In this case, the material is squeezed out onto the surface and filaments (threads) (fluff) are formed on the surface [34]. All these processes were manifested in our experiments

As a result of implantation of ion, an increase in hardness of up to 30% was obtained in the depth range of 0.5…3.5 μm [24]. The samples were irradiated with ions of helium with energy of 4 MeV. The hardness was $H_\mu \approx 440$ kg/mm^2. After irradiation, the surface of the materials had a different appearance from the unirradiated sample (Fig. 7,a).

When studying the images in Fig. 7,b,c, it was found that the structure of surface of the samples with different purity is different. Pits (craters) were found on the surface. These are points similar to point 1 (see Fig. 7,b,c). These pits indicate the occurrence of the flecking process [32, 34]. When irradiating the samples with ions of helium, bubbles are formed in tungsten [34]. We also observe protrusions (swellings, bubbles) on the surface. These are points similar to point 2 (see Fig. 7,b,c).

The processes of blistering are at work here. Because helium poorly dissolves in tungsten, then there is motion of bubbles to the surface. When they reach the surface, the bubbles burst. That is, the formation of pits is process of bursting of bubbles (removal of lid of bubbles). Therefore, processes of blistering should be considered as incomplete processes of flecking [32, 34]. We found that there are five times more pits than blisters. This result indicates a fairly high degree of destruction of surface of samples.

For the sample of tungsten of W-1 (99.5%), the number of peaks and craters is greater than for the sample of tungsten of W-n (99.7%) [24–27]. This is probably due to the amount of impurities. All these processes proceed in accordance with the theory of bubble appearance (formation) [32, 34], and have a coincidence with experimental results, got for steel [35].

When studying the structure of the samples, thin threads of tungsten (fluff) were found on the surface. These threads appeared when helium and deuterium ions exited the tungsten. These threads (fluff) grow in height and length with varying intensity. The growth rate depends on the intensity of irradiation [36, 37].

These are regions similar to region 3 (see Fig. 7,b). These threads (fluff) are formed as a result of exit of ions of helium from tungsten and the extrusion of atoms of tungsten [24–27]. An enlarged image of the region with fluff is shown in Fig. 8.

It was found that the length of the "fluff" was three times greater than its thickness [25–27]. In experimental works [36, 37] it was given that the height of the fluff was one and a half or two times greater than the thickness. This may be due to the fact that annealing effects took place. The growth of the "fluff" threads slows down due to effects of annealing,

a

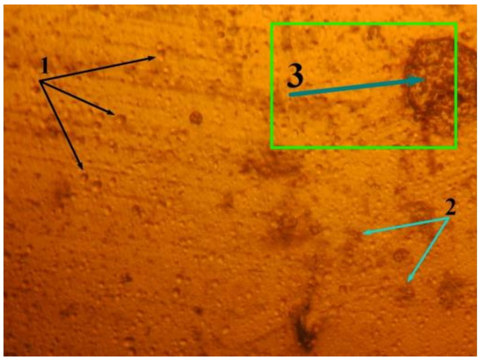

b

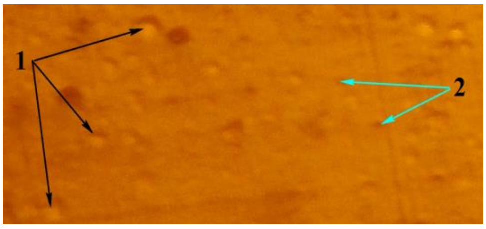

c

Fig. 7. Photographs of the surface of samples of tungsten: a – non-irradiated sample; b – irradiated sample W-1 (99.5%); c – irradiated sample W-n (99.7%) (1 – craters; 2 – peaks; 3 – "fluff"). Irradiation with ions of helium with energy 0.12 MeV

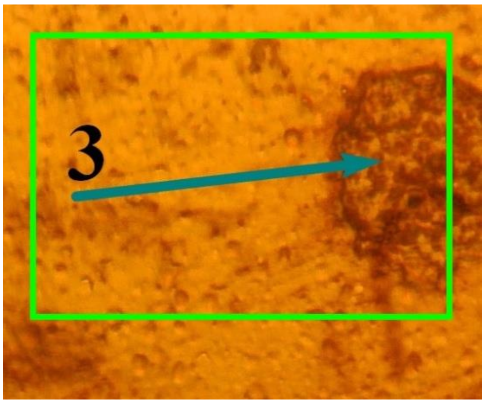

Fig. 8. Enlarged image of area of surface of samples of tungsten W-1 (99.5%), (3 – "fluff"). Irradiation with ions of helium with energy 0.12 MeV

This assumption is consistent with our results. In our case, the experimental temperature did not exceed 380 K. For the case of irradiation the ions of helium (of helium ion irradiation), the flecking effects and the "fluff" extrusion effects increase the rate of destruction of surface of tungsten (of the tungsten surface).

Note that, the destruction of surface of tungsten in our experiments we only have the effect of ions of helium at a temperature of 380 K. When calculating the speed destruction of surface, it is necessary to take into account the factor of the synergetic effect [38].

As a result of the impact of plasma flow and high temperatures on the surface of tungsten, the degree of destruction increases. At the same time, the coefficients of destruction are not simply summed up from each factor, but a synergistic effect is triggered, which increases the degree of destruction [38, 39].

The issue of resistance of the first wall of a thermonuclear reactor is far from being fully studied, so there remains a need for further study of this problem. Accordingly, our experimental and theoretical results are necessary.

CONCLUSIONS

1. High-purity samples of tungsten (99.5% (W-1) and 99.7% (W-n)) were irradiated with beams of ions of helium (E_{He^+} = 0.12 MeV and E_{He^+} = 4 MeV).

2. It was found that the processes of ionization, formation of phonons and vacancies occur to the depth of tungsten of 0.45 μm at E_{He^+} = 0.12 MeV and 6.8 μm at E_{He^+} = 4 MeV. It was shown that the change in these processes significantly depends on the energy of ions of helium. For high-purity samples of tungsten, the processes of ionization, formation of phonons and vacancies differ little from each other. The difference in the processes depended on the addition of molybdenum.

3. The profiles of coefficient of the displacement change over the depth of surface of layer of the tungsten were calculated. It was found that at an irradiation dose of $1·10^{18}$ ion/cm^2, the total displacement coefficients have the following values: dpa ≈ 60 for W-1 (99.5%), and dpa ≈ 59 for W-n (99.7%) at E_{He^+} = 0.12 MeV. For ions with energy E_{He^+} = 4 MeV, dpa ≈ 8.75 for W-1 (99.5%), and dpa ≈ 8.7 for W-n (99.7%).

4. A 30% increase in hardness was found in the depth range of 0.5…3.5 μm. The hardness was $H_μ$ ≈ 440 kg/mm^2 (E_{He^+} = 4 MeV).

5. It has been established that the flecking processes are five times more intense than the blistering processes, for the case of energies of ions of E_{He^+} = 0.12 MeV. This indicates to the exit of bubbles from tungsten.

6. It was found that the thickness of filaments of tungsten is three times less than their height. It testifies to the almost complete exit of ions of helium from material of tungsten.

7. It has been found that when the surface is exposed to radiation, plasma and high temperature, a synergistic effect occurs. This increases the speed of destruction of the first wall.

REFERENCES

1. T. Donné, W. Morris. European Research Roadmap to the Reaslisation of Fusion Energy // *EURO fusion.* September, 2018.

2. G. Federici et al. An Overview of the EU breeding blanket strategy as integral part of the DEMO design effort // *Fusion Eng. Des.* 2019, v. 141, p. 30-42.

3. M. Richardson et al. Technology readiness assessment of materials for DEMO in-vessel applications. // *J. Nucl. Mater.* 2021, v. 550, Article 152906.

4. H. You et al. High-heat-flux technologies for the European demo divertor targets: state-of-the-art and a review of the latest testing campaigns // *J. Nucl. Mater.* 2021, v. 544, Article 152670.

5. I.E. Garkusha et al. // *Fusion Sci. Technol.* 2014, v. 65(2), p. 186.

6. H. You et al. Limiters for DEMO wall protection: Initial design concepts & technology options // *Fusion Engineering and Design*. 2022, v. 174, p. 112988.

7. G. Pintsuk et al. Materials for in-vessel components // *Fusion Engineering and Design.* 2022, v. 174, p. 112994.

8. D. Stork et al. Developing structural, high-heat flux and plasma facing materials for a near-term DEMO fusion power plant: the EU assessment // *Journal of Nuclear Materials.* 2014, v. 455, p. 277-291.

9. M. Giménez, E. Lopasso. Tungsten carbide compact primary shielding for small medium reactor // *Ann. Nucl. Energy*. 2018, v. 116, p. 210-223.

10. S.N. Dubniuk, B.V. Zajtsev. The linear accelerator for radiation structural materials // *Problems of Atomic Science and Technology (PAST)*. 2014, N 3, p. 172-176.

11. R.A. Anokhin, B.V. Zaitsev, K.V. Pavlii, V.G. Zhuravlev, V.A. Soshenko. Experimental complex for investigation of construction materials on the helium ions linear accelerator // *PAST.* 2017, N 6(112), p. 167-171.

12. S.N. Dubniuk, R.A. Anokhin, A.F. Dyachenko, A.P. Kobets, A.I. Kravchenko, O.V. Manuilenko, K.V. Pavlii, V.N. Reshetnikov, A.S. Shevchenko, V.A. Soshenko, S.S. Tishkin, B.V. Zajtsev, A.V. Zhuravlyov, V.G. Zhuravlyov. Radiation complex on the basis of helium ions linac // *PAST.* 2018, N 4(116), p. 46-51.

13. I.M. Onishchenko, O.V. Manuilenko, B.V. Zajtsev, S.M. Dubniuk, A.P. Kobets, A.I. Kravchenko, K.V. Pavlii, V.M. Reshetnikov, V.A. Soshenko, S.S. Tishkin, O.V. Zhuravlyov, V.G. Zhuravlyov. Experimental research and work development on the helium ions linac // *PAST*. 2021, N 6(136), p. 197-200; https://doi.org/10.46813/2021-136-197

14. E.M. Prohorenko, V.F. Klepikov, V.V. Lytvynenko, N.I. Bazaleyev, I.I. Magda, T.G. Prohorenko, A.I. Morozov. Application of ir-radiometric diagnostics for control of vacuum connections of electrophysical installations // *PAST.* 2018, N 1(113), p. 212-217.

15. V.F. Klepikov, E.M. Prokhorenko, V.V. Lytvynenko, S.E. Donets, V.N. Robuk, T.G. Prokhorenko, V.T. Uvarov, A.G. Ponomarev, Yu.F. Lonin. The use of high-current relativistic electron beams for the study of the effects of ionizing radiation on materials storage RAW // *PAST.* 2016, N 2(102), p. 72-77.

16. R. Neu et al. Tungsten fibre-reinforced composites for advanced plasma facing components. // *Nucl. Mater. Energy.* 2017, v. 12, p. 1308-1313.

17. E.M. Prohorenko, V.V. Lytvynenko, A.A. Zaharchenko, M.A. Hazhmuratov, T.G. Prokhorenko. Studying the changes in the characteristics of radiation-

protective composition materials in dependence on homogeneity of distributing of metal components // *PAST*. 2019, N 2(120), p. 121-126.

18. E.M. Prohorenko, V.V. Lytvynenko, A.A. Zaharchenko, M.A. Hazhmuratov, S.A. Sokolov, T.G. Prokhorenko, A.P. Ben. Analysis of radiation protective properties of polystyrene – based composite materials // *PAST*. 2021, N 3(133), p. 111-118; https: //doi.org/ 10.46813/ 2021-133-111

19. E.M. Prohorenko, V.V. Lytvynenko, A.A. Zaharchenko, M.A. Hazhmuratov, T.G. Prokhorenko. Study of strength characteristics and radiation protective properties of polystyrene tungsten composite materials // *PAST*. 2023, N 2(144), p. 29-36; https: //doi.org/ 10.46813/ 2023-144-029

20. Y. Mao et al. Design of tungsten fiber-reinforced tungsten composites with porous matrix // *Mater. Sci. Eng. A*. 2021, v. 817, Article 141361.

21. E. Prokhorenko, V. Klepikov, V. Lytvynenko, N. Shul'gin, A. Morozov. Diagnostics of processes of wear of materials of ball-tube mills // *Eastern European Journal of Enterprise Technologie*. 2015, N 1/5, v. 73, p. 14-20.

22. E.M. Prokhorenko, V.V. Lytvynenko, O.A. Melyakova, Yu.F. Lonin, A.G. Ponomarev, V.T. Uvarov, N.A. Shul'gin, T.G. Prokhorenko, R.I. Starovoytov, A.I. Morozov, S.R. Artemev. Strengthening of the surface of steel (9XFM) exposed to a high-current electron beam // *PAST*. 2020, N 1(125), p. 167-172.

23. E.M. Prokhorenko, V.V. Lytvynenko, O.A. Melyakova, Yu.F. Lonin, A.G. Ponomarev, V.T. Uvarov, N.A. Shul'gin, T.G. Prokhorenko. Modification of structure of the surface of steel (XGC) as result of influences of high-current electron beam // *PAST*. 2020, N 2(126), p. 47-53.

24. O.V. Manuilenko, E.M. Prokhorenko, K.V. Pavlii, B.V. Zajtsev, S.N. Dubniuk, V.V. Lytvynenko, T.G. Prokhorenko. Changes of the radiation characteristics of surface of tungsten as a result of influence of helium ion beams // *PAST*. 2022, N 3(139), p. 36-41; https: //doi.org/ 10.46813/ 202-139-36

25. O.V. Manuilenko, E.M. Prokhorenko, K.V. Pavlii, B.V. Zajtsev, S.N. Dubniuk, V.V. Lytvynenko, T.G. Prokhorenko. Influence of helium ions beams with energies 0.12 MeV on sputtering process on surface of tungsten // *PAST*. 2023, N 3(145), p. 158-163; https: //doi.org/ 10.46813/ 2023-145-158

26. O.V. Manuilenko, E.M. Prokhorenko, K.V. Pavlii, B.V Zajtsev, S.N. Dubniuk, V.V. Lytvynenko, T.G. Prokhorenko. Features of structural damages of surface of tungsten as a result of irradiation with helium ion beams with energy 4 MeV // *PAST*. 2023, N 6(148), p. 33-38; https: //doi.org/10.46813/ 2023-148-033

27. O.V. Manuilenko, E.M. Prokhorenko, K.V. Pavlii, B.V. Zajtsev, V.A. Soshenko, V.I. Butenko, T.G. Prokhorenko. Comparison of structural disruptions on the tungsten surfaces which induced by irradiation of helium ions beams with energies 0.12 and 4 MeV // *PAST*. 2024, N 3(151), p. 117-123; https://doi.org/10.46813/2024-151-117

28. M.R. Gilbert, K. Arakawa, et al. Perspectives on multiscale modeling and experiments to accelerate materials development for fusion // *Journal of Nuclear Materials*. 2021, v. 554, p. 153113.

29. http://www.srim.org.

30. E.M. Prokhorenko, V.V. Lytvynenko, A.A. Zakharchenko, M.A. Khazhmuradov, S.A. Sokolov, T.G. Prokhorenko, A.P. Ben. Brief overview on research and development of radiation shielding protective composite materials based on polystyrene // *PAST*. 2024, N 2(150), p. 107-114.

31. Suchandrima Das, Hongbing Yu, et al. Hardening and Strain Localisation in Helium-Ion-Implanted Tungsten // www.nature.com/ Scientific Reports, 2019, 9:18354; https://doi.org/10.1038/s41598-019-54753-3

32. S. Sharafat et al. A description of stress driven bubble growth of helium implanted tungsten // *J. Nucl. Mater*. 2009, v. 389, p. 203-212; https://doi.org/10.1016/j.jnucmat.2009.02.027

33. P. Fiflis, D. Curreli, D.N. Ruzic. Direct time-resolved observation of tungsten nanostructured growth due to helium plasma exposure // *Nucl. Fusion*. 2015, v. 55, p. 033020 (7 p.).

34. M. Gago et al. Bubble Formation in ITER-Grade Tungsten after Exposure to Stationary D/He Plasma and ELM-like Thermal Shocks // *J. Nucl. Eng*. 2023, v. 4(1), p 204-212; https://doi.org/10.3390/jne4010016

35. I.V. Kolodiy, O.S. Kalchenko, M.A. Tikhonovsky, G.D. Tolstolutska. Effect of inert gas ions irradiation on radiation damage of high-entropy alloy CrFe2MnNi and 18Cr10NiTi steel // *PAST*. 2025, N 2(156), p. 3-11; https: //doi.org/ 10.46813/ 2025-156-003

36. S. Takamura, N. Ohno, et al. Formation of Nanostructured Tungsten with Arborescent Shape due to Helium Plasma Irradiation // *Plasma and Fusion Research: Rapid Communications*. 2006, v. 1, p. 051.

37. M. Baldwin, R. Doerner. Helium induced nanoscopic morphologhy on tungsten under fusion relevant plasma conditions // *Nucl. Fusion*. 2008, v. 48, 035001–5.

38. N. Lemahieu et al. Synergistic effects of ELMs and steady state H and H/He irradiation on tungsten // *Fusion Engineering and Design*. 2015, v. 98-99, p. 2020-2024.

39. V.A. Makhlai, I.E. Garkusha, et al. Irradiation of sintered tungsten samples with combined helium ion beam and high-heat fluxes of qspa hydrogen plasma // *PAST*. 2025, N 1(155), p. 75-78.

Article received 03.04.2025

ПОРУШЕННЯ СТРУКТУРИ ПОВЕРХНІ ЗРАЗКІВ ВОЛЬФРАМУ ЧИСТОТОЮ 99,5 І 99,7%, ЯКІ БУЛИ ОПРОМІНЕНІ ІОНАМИ ГЕЛІЮ З ЕНЕРГІЄЮ 0,12 АБО 4 МеВ

Є.М. Прохоренко, О.В. Мануйленко, І.М. Оніщенко, В.В. Литвиненко, Б.В. Зайцев, К.В. Павлій, В.А. Сошенко, В.І. Бутенко, Т.Г. Прохоренко

Вольфрам високої чистоти (99,7% (W-n) і 99,5% (W-1)) розглядався як матеріал для створення першої стінки термоядерного реактора. Вибір вольфраму як перспективного матеріалу першої стінки визначався його високими термостійкими характеристиками, низькою корозійністю, високою радіаційною стійкістю. Для розуміння впливу опромінення на властивості та характеристики високочистого вольфраму та порівняння з керамічними матеріалами та матеріалами із спеціальних сортів сталі, виконано опромінення зразків вольфраму іонами гелію з енергіями $E_{He}{}^{+}$ = 0,12 МеВ або $E_{He}{}^{+}$ = 4 МеВ. Досліджено зміну структурних порушень поверхні. Знайдено, що процеси флекінгу протікають у п'ять разів інтенсивніше, ніж процеси блістерингу. Також виявлено, що при утворенні вольфрамового пуху товщина окремих ниток у три рази менша за висоту. Методами математичного моделювання пораховано коефіцієнти іонізації, генерації фононів та виникнення вакансій. Знайдено коефіцієнти дефектоутворення по глибині проникнення іонів гелію у вольфрам, а також сумарні коефіцієнти зміщень залежно від енергії опромінення.